



SPE 56691

## Effect of Pressure Uncertainty on Material-Balance Plots

Mark P. Walsh, SPE, Petroleum Recovery Research Institute

Copyright 1999, Society of Petroleum Engineers, Inc.

This paper was prepared for presentation at the 1999 SPE Annual Technical Conference and Exhibition held in Houston, Texas, 3–6 October 1999.

This paper was selected for presentation by an SPE Program Committee following review of information contained in an abstract submitted by the author(s). Contents of the paper, as presented, have not been reviewed by the Society of Petroleum Engineers and are subject to correction by the author(s). The material, as presented, does not necessarily reflect any position of the Society of Petroleum Engineers, its officers, or members. Papers presented at SPE meetings are subject to publication review by Editorial Committees of the Society of Petroleum Engineers. Electronic reproduction, distribution, or storage of any part of this paper for commercial purposes without the written consent of the Society of Petroleum Engineers is prohibited. Permission to reproduce in print is restricted to an abstract of not more than 300 words; illustrations may not be copied. The abstract must contain conspicuous acknowledgment of where and by whom the paper was presented. Write Librarian, SPE, P.O. Box 833836, Richardson, TX 75083-3836, U.S.A., fax 01-972-952-9435.

### Abstract

Straight-line material-balance plots are routinely used to analyze reservoir performance and estimate the OOIP and OGIP. Application necessarily requires average reservoir pressure measurements. Invariably, these measurements are subject to error. This paper presents a statistical analysis of the effects of pressure uncertainty on the practical applicability of these plots.

Results reveal that pressure uncertainty can drastically affect the reliability of certain plots. While all proposed plots are theoretically valid, certain plots are practically and categorically flawed because they require virtually error-free pressure measurements—a practical impossibility. The problem is further exacerbated by the observation that flawed and valid plots alike yield the same apparent linear character. This observation has lulled practitioners into a false sense of confidence that the flawed plots are meaningful and applicable. The plots are ultimately classified in terms of their error tolerance and sensitivity. The hypersensitive plots should be avoided.

### Introduction

Straight-line, material-balance plots are routinely used to analyze reservoir performance. Among other things, these plots are used to estimate the OOIP and OGIP. Havlena and Odeh<sup>1</sup> proposed numerous plots, each applicable to a unique reservoir situation. Their plots included the  $F$ -vs.- $E_o$  plot for initially-undersaturated oil reservoirs and the  $F/E_o$ -vs.- $E_g/E_o$  and  $F$ -vs.- $(E_o + mB_{oi}E_g/B_{gi})$  plots for initially-saturated reservoirs.

While all such plots are theoretically valid, not all are practically valid owing to data uncertainty. Since data uncertainty is unavoidable and inevitable, its effects are important. Data uncertainty includes error in the measurement of laboratory PVT properties, field production data and average reservoir pressures. Of these sources of error, pressure uncertainty is perhaps the most serious.

Several investigators have observed the problems caused by pressure uncertainty. McEwen<sup>2</sup> was among the first, and he

noted that Havlena and Odeh's method of plotting  $F/E_o$  vs.  $\Sigma \Delta p W_D/E_o$  to simultaneously determine the OOIP and aquifer constant in initially-undersaturated, water-drive oil reservoirs was unreliable if there was much pressure uncertainty. To improve the tolerance, he recommended plotting  $F$  vs.  $E_{ow}$ , where

$$E_{ow} = E_o + \frac{2B_{oi}c_t \Sigma \Delta p W_D}{1 - S_{wi}} \quad (1)$$

for radial aquifers. Tehrani<sup>3</sup> and Wang and Hwan,<sup>4</sup> too, have noted the problems caused by pressure uncertainty in water-drive reservoirs and have rendered important observations.

Unfortunately, very few investigators have examined the effects of pressure uncertainty on material-balance plots for other types of reservoirs, especially volumetric reservoirs. Volumetric reservoirs may be initially undersaturated or saturated; initially-saturated reservoirs include gas-cap reservoirs. The work by Wang and Hwan (1997) included a brief examination of volumetric gas-cap reservoirs. They showed an example where the method of plotting  $F/E_o$  vs.  $E_g/E_o$  exhibited a greater error in estimating the OOIP than a non-graphical, iterative method which sought to minimize the "pressure standard deviation." Their investigation, however, did not report the error sensitivity as a function of uncertainty or gas-cap size. Nor did they investigate the other important plots for volumetric reservoirs.

This work presents a systematic and comprehensive statistical analysis of the effect of pressure uncertainty on the reliability of material-balance plots to determine the OOIP and OGIP in volumetric reservoirs. Specifically, we examine the following material-balance methods: (1)  $F$  vs.  $E_o$ , (2)  $F/E_o$  vs.  $E_g/E_o$ , (3)  $F/E_o$  vs.  $(E_o + mB_{oi}E_g/B_{gi})$  and (4) least-squares planar regression. The first three of these methods routinely employ least-squares linear regression. The first method is applicable to initially-undersaturated oil reservoirs while the last three are applicable to initially-saturated reservoirs.

Uncertainty is introduced by assuming the error in the pressure measurements is random and normally distributed. Ten different normalized error realizations are considered to ensure representative sampling. Pressure errors in the range 0 to 200 psi are considered. In addition, the effect of gas-cap size is considered. In total, over 400 separate OOIP and OGIP calculations are carried out to characterize the effect of pressure uncertainty.

Our analysis reveals that certain plots are especially tolerant of uncertainty while others are flawed owing to hypersensitivity. The hypersensitive plots should be avoided.

### Material-Balance Plots.

Havlena and Odeh proposed the following plots for volumetric reservoirs:

1.  $F$  vs.  $E_o$  for initially-undersaturated oil reservoirs;
2.  $F/E_o$  vs.  $E_g/E_o$  for initially-saturated reservoirs;
3.  $F$  vs.  $(E_o + mB_{oi}E_g/B_{gi})$  for initially-saturated reservoirs.

The variables  $F$ ,  $E_o$ , and  $E_g$  are defined in the appendix. The definitions therein are based on the generalized material-balance equation of Walsh<sup>5,6</sup> and not on the conventional material-balance equation used by Havlena and Odeh.<sup>1</sup> The advantage of the former is that the plots herein are applicable to the full range of reservoir fluids—including volatile oils and gas condensates—whereas the latter limits application to only black oils and dry gases.

**$F$ -vs.- $E_o$  Plots.** Eqn. (A-9) reveals that the slope of an  $F$ -vs.- $E_o$  plot yields the OOIP. If least-squares linear regression is applied, the OOIP is given by

$$N = \frac{n\sum yx - \sum y\sum x}{n\sum x^2 - \sum x\sum x} \quad (2a)$$

and the y-intercept of the line  $y = a + bx$  is

$$a = \frac{\sum y - N\sum x}{n} \quad (2b)$$

where  $y$  and  $x$  are the dependent and independent variables, respectively, and defined by

$$y = F \quad (2c)$$

$$x = E_o \quad (2d)$$

and  $n$  is the number of data points. Eqn. (2) uses the notation that

$$\sum x = \sum_{i=1}^n x_i \quad (3)$$

Eqn. (2) does not restrict the line to pass through the origin. If one however demands that the least-squares line pass through the origin, then the OOIP is given by

$$N = \frac{\sum y}{\sum x} \quad (4)$$

where the definitions for  $y$  and  $x$  in (2c) and (2d) apply.

Given the OOIP, the OGIP can easily be determined and is given by the product of the OOIP and the initial dissolved gas-oil ratio.

This method is entirely analogous to plotting  $F$  vs.  $E_g$  or  $p/z$  vs.  $G_p$  for dry-gas reservoirs.

**$F/E_o$ -vs.- $E_g/E_o$  Plot.** If one divides (A-1) by  $E_o$ , the resulting equation reveals that a plot of  $F/E_o$  vs.  $E_g/E_o$  yields a straight line with a slope equal to  $G_{fgi}$  and a y-intercept equal to  $N_{foi}$ . If least-squares linear regression is applied, then

$$G_{fgi} = \frac{n\sum yx - \sum y\sum x}{n\sum x^2 - \sum x\sum x} \quad (5a)$$

$$N_{foi} = \frac{\sum y - G_{fgi}\sum x}{n} \quad (5b)$$

where  $y$  and  $x$  are defined by

$$y = \frac{F}{E_o} \quad (5c)$$

$$x = \frac{E_g}{E_o} \quad (5d)$$

For the case of a black oil, the volatilized-oil content of the reservoir gas phase is negligible and it follows that  $N_{foi} = N$ .

**$F$ -vs.- $(E_o + mB_{oi}E_g/B_{gi})$  Plot.** Eqn. (A-8) reveals that a plot of  $F$  vs.  $(E_o + mB_{oi}E_g/B_{gi})$  yields a straight line with a slope equal to  $N_{foi}$ . Application of least-squares regression yields

$$N_{foi} = \frac{n\sum yx - \sum y\sum x}{n\sum x^2 - \sum x\sum x} \quad (6a)$$

where  $y$  is given by (2c) and  $x$  is

$$x = E_o + \frac{mB_{oi}E_g}{B_{gi}} \quad (6b)$$

Since  $m$  is generally treated as an unknown, the simultaneous solution for  $m$  and  $N_{foi}$  is not direct but iterative. Iteration is needed to determine the value of  $m$  which minimizes the non-linearity, i.e., material-balance error.

The solution procedure to solve for  $m$  and  $N_{foi}$  is as follows:

1. Guess  $m$ .
2. Compute  $N_{foi}$  using (6a).
3. Compute the sum of the squares of the withdrawal deviation (SSWD) from

$$SSWD = \sum_{i=1}^n (y_i - N_{foi}x_i)^2 \quad (7)$$

where  $y$  and  $x$  are defined by (2c) and (6b), respectively.

4. Is SSWD a minimum?
5. If no, return to Step 1; if yes, terminate.

This procedure requires a minimization routine. We employ a generalized reduced gradient technique.<sup>7</sup>

**Planar (Multivariate) Regression.** We consider a fourth method to determine the OOIP and OGIP. If we apply least-squares planar regression to (A-1), we obtain

$$G_{fgi} = \frac{\Sigma yz - \frac{\Sigma z \Sigma y}{n} - \frac{[\Sigma zx - \frac{\Sigma z \Sigma x}{n}][\Sigma xy - \frac{\Sigma x \Sigma y}{n}]}{[\Sigma x^2 - \frac{\Sigma x \Sigma x}{n}]} \quad (8a)$$

$$\frac{[\Sigma y \Sigma x - \Sigma xy][\Sigma xy - \frac{\Sigma x \Sigma y}{n}]}{[\Sigma x^2 - \frac{\Sigma x \Sigma x}{n}]} + \Sigma y^2 - \frac{\Sigma y \Sigma y}{n}$$

$$N_{foi} = \frac{\Sigma zx - \frac{\Sigma z \Sigma x}{n} + G_{fgi} \left[ \frac{\Sigma x \Sigma y}{n} - \Sigma xy \right]}{\Sigma x^2 - \frac{\Sigma x \Sigma x}{n}} \quad (8b)$$

where  $z$ ,  $x$ , and  $y$  are given by

$$z = F \quad (8c)$$

$$x = E_o \quad (8d)$$

$$y = E_g \quad (8e)$$

This method contrasts the previous three, which are based on least-squares linear regression. The graphical interpretation of this method is that it finds the least-squares plane in a three-dimensional space defined by the axes  $x$ ,  $y$  and  $z$ . This method basically follows from the recommendations of Tehrani.<sup>3</sup>

Other forms of (2a), (2b), (5a), (5b), (6a), (8a), and (8b) are possible; however, we purposely choose these forms because they are especially convenient for spreadsheet calculations.

### Approach

Our approach is to consider partially-depleted, hypothetical reservoirs of known OOIP and OGIP and with given production histories; to introduce uncertainty into the dynamic average reservoir pressure measurements; and then to estimate the OOIP and OGIP using the material-balance methods outlined herein. Our analysis investigates the effect of pressure uncertainty and gas-cap size on the reliability of the material-balance methods.

Although our work is limited to an investigation of uncertainty by pressure errors, the effect of uncertainty from other variables such as PVT properties and cumulative production measurements is expected to be similar.

### Idealized Reservoir

Table 1 summarizes the properties of the hypothetical reservoirs. Three reservoirs are considered, each identical except for different gas-cap sizes. The gas-cap size is characterized in terms of the ratio of the initial free-gas to free-oil phase volumes,  $m$ . Three reservoirs with values of  $m = 0, 0.25$  and  $0.50$  are considered. Reservoirs with values of  $m$  greater than  $0.50$  were considered; however, a reporting of these results was not material.

Each hypothetical reservoir had a OOIP of 100 mmstb. The original free-gas inplace (OFGIP) varied between 0 and 38 Bscf; the total OGIP varied between 82 and 120 Bscf.

The PVT properties for each reservoir are shown in Table 2. The same PVT properties applied to each reservoir. The properties in Table 2 simulate those of a well-known West Texas black-oil reservoir.

The pressure dependence of the PVT properties exactly fit the following equations:

$$B_o(p) = 1.123 \left[ 10^{6.986 \times 10^{-5} p} \right] \quad (9)$$

$$R_s(p) = 294.4 \left[ 10^{2.715 \times 10^{-4} p} \right] \quad (10)$$

$$B_g(p) = (7.9803 \times 10^{-3}) - (6.1666 \times 10^{-6}) p + (1.509 \times 10^{-9}) p^2 \quad (11)$$

Table 3 summarizes the applicable production histories. This data was computed with a reservoir simulator.<sup>8</sup> The data in Table 3 exactly balances material. Pressure depletion was carried out from 1,640 to 1,000 psia. The oil and gas recoveries increase with gas-cap size, as expected.

### Pressure Uncertainty

Galas<sup>9</sup> has reported an estimated average pressure uncertainty of at least 10 to 50 psi, depending on the method of measurement and reservoir conditions. Uncertainties as high as 100 psi were not unusual.

Pressure uncertainty was statistically introduced into the "true" average reservoir pressure measurements by assuming the error was random and normally distributed. The magnitude of the pressure error is effectively characterized in terms of the standard deviation and standard error of each distribution.

Ten different normalized error realizations were considered so as to ensure representative sampling. The normalized error is defined as the quotient of the error and the standard deviation. Table 4 shows the ten realizations used in this work. Each realization consisted of 15 data points. Each data point corresponded to one of the pressures listed in Table 3. The data was computed using a random number generator. The actual and idealized standard deviations differed slightly owing to finite sampling. The actual standard deviations varied from 0.540 to 1.353. The average of all ten realizations was 0.948, indicating a representative normal distribution overall. A histogram of the normalized error confirmed the normal distribution.

The "actual" pressure was determined by adding the product of the normalized error and the applicable standard deviation to the "true" pressure. Table 5 shows the results for a standard deviation of 5 psi. Notice that the actual pressures are sometimes greater than and less than the true pressures. This is an expected feature of a random distribution.

### Results

**F-vs.- $E_o$  Plot.** Table 6 and Fig. 1 summarize the effect of pressure uncertainty on the reliability of the  $F$ -vs.- $E_o$  plot to determine the OOIP. Pressure uncertainties between 0 and 200 psi were considered. For each uncertainty, the OOIP and its

error was computed for each of the ten realizations; then the average error of all ten realizations was computed.

Two methods were used to compute the OOIP: (1) the unrestricted least-squares line and (2) the least-squares line which passed through the origin. The results of the former method are tabulated in the second column (labelled  $y = a + bx$ ) in Table 6. The results of the latter method are placed in the third column and labelled  $y = bx$ . The former method uses (2) and the latter method uses (4).

Both methods yield comparable results. Thus, one method does not appear to yield better tolerance to pressure uncertainty over the other. Most importantly, both methods yield good tolerance. For example, the two methods yield errors of only 7.4 and 9.4% for an uncertainty of 50 psi. An uncertainty of 50 psi is considered relatively moderate and typical. Even at an uncertainty of 100 psi, the error is quite tolerable and is only 15.4 and 16.7%.

Figure 2 illustrates the  $F$ -vs.- $E_o$  plot for the case of Realization #10, and an uncertainty of 50 psi. The solid line represents the least-squares line; the slope of the line is 91.5 mmstb, and this value equals the estimated OOIP. The error in estimating the OOIP was 8.5%. The other realizations yielded similar results. The scatter of the data in Fig. 2 is considered representative of field cases. The scatter increases with uncertainty.

Our analysis concludes that the method of plotting  $F$  vs.  $E_o$  exhibits good tolerance to pressure uncertainty. Since  $F$ -vs.- $E_o$  plots for oil reservoirs are equivalent to  $F$ -vs.- $E_g$  and  $p/z$ -vs.- $G_p$  plots for gas reservoirs, the conclusions tendered here are likewise applicable to these latter plots.

**$F/E_o$ -vs.- $E_g/E_o$  Plot.** Table 7 and Fig. 3 summarize the effect of pressure uncertainty on the reliability of a  $F/E_o$ -vs.- $E_g/E_o$  plot. Our analysis included the effect of gas-cap size. The results reveal hypersensitivity to uncertainty. For example, the error in estimating the OOIP is in excess of 100% if the pressure uncertainty is only 5 psi, regardless of the gas-cap size. The effect of increasing the gas cap serves to only increase the error.

Note that the error is zero if the uncertainty is 0 psi. This reveals that this method yields error-free estimates in the absence of uncertainty. This fact establishes the theoretical correctness of the method. However, the error increases rapidly with only small amounts of uncertainty. Table 7 reveals that the uncertainty must be less than 1 psi to realize an error less than 20%. This means that virtually error-free pressure measurements—a practical impossibility—are needed to yield acceptable results. These facts establish the hypersensitivity of the method.

Table 7 includes the errors in estimating the OFGIP (original free-gas inplace) and total OGIP. The former quantity is computed directly from the slope of the  $F/E_o$ -vs.- $E_g/E_o$  plot. In contrast, the latter quantity is computed indirectly and is given by the following equation:

$$G = G_{f_{gi}} + N_{f_{oi}}R_{si} \quad (12)$$

where  $G$  is the OGIP,  $G_{f_{gi}}$  is the OFGIP, and the product  $N_{f_{oi}}R_{si}$  is the original dissolved-gas inplace.

The results reveal that the estimates of the OFGIP and OGIP, too, are hypersensitive to the uncertainty, although the latter quantity is less sensitive than the former.

Fig. 4 illustrates the  $F/E_o$ -vs.- $E_g/E_o$  plot for the case of Realization #7, a pressure uncertainty of only 2 psi, and for  $m = 0.25$ . The solid line represents the least-squares line. The line exhibits a y-intercept and slope of 47 mmstb and 48 Bscf, respectively. These values correspond to the estimated OOIP and OFGIP, respectively. In comparison, the actual OOIP and OFGIP are 100 mmstb and 19 Bscf, respectively. The method yields OOIP and OFGIP errors of 53 and 151%, respectively. These errors are substantial and reflect hypersensitivity.

Note the relatively linear nature of the data in Fig. 4. The lack of obvious non-linearity might lull one into a false sense of confidence that the method is applicable and yields acceptable predictions; this, of course, is not correct. We conclude that the presence of obvious non-linearity is neither a necessary nor a sufficient condition to reliably identify erroneous predictions.

Graphically, the problem with this method is that it compresses the data to within a relatively small region. This, in turn, yields large errors in the slope and y-intercept if uncertainty is present.

The sensitivity of the  $F/E_o$ -vs.- $E_g/E_o$  plot is so severe that it is not uncommon for the method to predict the presence of a sizable gas cap when none exists. For example, for Realization #7 and an uncertainty of only 2 psi, the method predicts a gas cap corresponding to  $m = 0.48$  when none exists. The corresponding  $F/E_o$ -vs.- $E_g/E_o$  plot again exhibits reasonably linear character, similar to that in Fig. 4.

The hypersensitivity of this plot appears to be analogous to the hypersensitivity of the  $F/E_o$ -vs.- $(\Sigma \Delta p W_D)/E_o$  plot noted by Tehrani<sup>3</sup> for water-drive reservoirs. In his case, he claimed the problem was caused by reducing the number of independent variables. This occurred when one of the independent variables ( $\Sigma \Delta p W_D$ ) and the dependent variable ( $F$ ) were divided by the remaining independent variable ( $E_o$ ). Tehrani referred to this problem as a loss in “resolving power.”

**$F$ -vs.- $(E_o + mB_{oi}E_g/B_{gi})$  Plot.** Table 8 and Fig. 5 summarize the results of  $F$ -vs.- $(E_o + mB_{oi}E_g/B_{gi})$  plot. The error in estimating the OOIP, OFGIP and OGIP is reported as a function of the uncertainty and the gas cap size. The results show that this plot, too, is hypersensitive to the uncertainty; however, the sensitivity is less than that of the  $F/E_o$ -vs.- $E_g/E_o$  plot. For example, the average error in estimating the OOIP is 37.5% for the case of an uncertainty of 5 psi and  $m = 0$ . In comparison, the average error is 124% for the same case for the  $F/E_o$ -vs.- $E_g/E_o$  plot. Although the error is less, it rapidly increases with uncertainty. For example, the error increases from 37.5 to 59.3% as the uncertainty increases from 5 to 10 psi. Because uncertainty is typically greater than 10 psi, these results suggest hypersensitivity.

Table 8 shows that the error in estimating the OFGIP is greater than the error in estimating the OOIP. Note, however, that the error in estimating the OGIP is much less, approaching possibly acceptable levels. For example, the average error in estimating the OOIP, OFGIP and OGIP is 49.9, 139.9, and 14.2%, respectively, for the case of an uncertainty of 5 psi and  $m = 0.25$ . Although the error in estimating the OGIP is much less, we question the reliability of such estimates since they are exclusively based on the OOIP and OFGIP estimates, both of which are very unreliable and often highly erroneous.

Fig. 6 illustrates the  $F$ -vs.- $(E_o + mB_{oi}E_g/B_{gi})$  plot for the case of Realization #4, an uncertainty of only 5 psi, and  $m = 0.25$ . The iterative solution method yields  $m = -0.10$  when the material-balance error is minimized. The solid line represents the least-squares line. This line yields a slope of 160 mmstb. This value corresponds to the estimated OOIP. In comparison, the actual OOIP is 100 mmstb. The method yields an error of 60%. This error is quite substantial, especially in view of the fact that the uncertainty is only 5 psi.

Note the linear character of the data in Fig. 6. The correlation coefficient exceeds 0.999. This linearity exists despite a grossly erroneous OOIP estimate. This illustrates that the linearity of the plot cannot be used as a reliable indicator of the plot's applicability. Thus, one should not let the linearity of the plot lull one into a false sense of confidence that the resulting OOIP estimate is good. Incidentally, the linearity of the plot in Fig. 6 is characteristic of most of the plots we constructed.

**Planar (Multivariate) Regression.** Table 9 and Fig. 7 summarize the results of planar regression. Table 9 reports the error in estimating the OOIP, OFGIP and OGIP as a function of the uncertainty and gas-cap size ( $m$ ). The results of planar regression are very similar to the  $F$ -vs.- $(E_o + mB_{oi}E_g/B_{gi})$  plot; however, the former method has the distinct advantage of a direct solution while the latter method requires an iterative solution.

Although planar regression and the  $F$ -vs.- $(E_o + mB_{oi}E_g/B_{gi})$  plot yield comparable errors when averaging the results of the ten realizations, the error of each method may differ for individual cases. For example, planar regression yields OOIP, OFGIP and OGIP estimates of 130.8 mmstb, 3.7 Bscf, and 111 Bscf, respectively, while the  $F$ -vs.- $(E_o + mB_{oi}E_g/B_{gi})$  plot yields estimates of 160 mmstb, -12.1 Bscf, and 119.5 Bscf, respectively, for the case of Realization #1, an uncertainty of 5 psi, and  $m = 0.25$ . In comparison, the actual OOIP, OFGIP, and OGIP are 100 mmstb, 19.98 Bscf, and 100.98 Bscf, respectively. In this example, planar regression yields slightly better estimates than the  $F$ -vs.- $(E_o + mB_{oi}E_g/B_{gi})$  plot. In other examples, the latter method yields slightly better estimates.

## Summary and Conclusions

1. The method of plotting  $F$  vs.  $E_o$  for initially-undersaturated, volumetric oil reservoirs exhibits good tolerance to pressure uncertainty.
2. The method of plotting  $F/E_o$  vs.  $E_g/E_o$  for initially-saturated, volumetric reservoirs exhibits poor tolerance to pressure uncertainty. This method is not recommended.
3. The method of plotting  $F$  vs.  $(E_o + mB_{oi}E_g/B_{gi})$  for initially-saturated, volumetric reservoirs exhibits poor tolerance to pressure uncertainty. This method, however, exhibits slightly better tolerance than the method of plotting  $F/E_o$  vs.  $E_g/E_o$ .
4. The method of planar regression for initially-saturated, volumetric reservoirs exhibits uncertainty tolerance comparable to the method of plotting  $F$  vs.  $(E_o + mB_{oi}E_g/B_{gi})$ . The former method is preferred over the latter because the former offers a direct solution while the latter requires an iterative solution.
5. None of the material-balance methods for initially-saturated, volumetric reservoirs exhibit good tolerance.

6. The methods of plotting  $F/E_o$  vs.  $E_g/E_o$  and  $F$  vs.  $(E_o + mB_{oi}E_g/B_{gi})$  yield highly erroneous OOIP estimates despite yielding remarkably linear plots. Thus, a plot's linearity cannot be used as a reliable indicator of its applicability.

## Nomenclature

$a$  = constant

$b$  = constant

$B_g$  = gas FVF, rb/mscf

$B_{gi}$  = initial gas FVF, rb/mscf

$B_{oi}$  = Initial oil FVF, rb/stb

$B_o$  = oil FVF, rb/stb

$B_{to}$  = two-phase oil FVF, rb/stb

$B_{tg}$  = two-phase gas FVF, rb/stb

$B_w$  = water FVF, rb/stb

$c_t$  = total compressibility, psi<sup>-1</sup>

$E_g$  = gas expansivity, rb/mscf

$E_{ow}$  = expansivity defined by Eqn. (1), rb/stb

$E_o$  = oil expansivity, rb/stb

$F$  = net fluid withdrawal, rb

$G$  = original gas inplace, scf

$G_{fgi}$  = original free gas inplace, scf

$G_{ps}$  = cumulative produced sales gas, scf

$G_p$  = cumulative produced wellhead gas, scf

$m$  = ratio of initial free-gas to free-oil phase volume

$n$  = total number of data points

$N$  = original oil inplace, stb

$N_{foi}$  = original free oil inplace, stb

$p$  = pressure, psi

$\Delta p$  = initial minus prevailing pressure, psi

$R_s$  = dissolved gas-oil ratio, scf/stb

$R_{si}$  = initial dissolved gas-oil ratio, scf/stb

$R_v$  = volatilized oil-gas ratio, stb/scf

$R_{vi}$  = initial volatilized oil-gas ratio, stb/scf

$S_{wi}$  = initial water saturation, fraction

$W_D$  = dimensionless water influx

$W_i$  = cumulative injected water, stb

$W_p$  = cumulative produced water, stb

$x$  = independent variable

$y$  = independent or dependent variable

$z$  = z-factor or dependent variable

## References

1. Havlena, D. and Odeh, A.S.: "The Material Balance Equation as an Equation of a Straight Line," J. Pet. Tech. (Aug., 1963); Trans. AIME 228.
2. McEwen, C.R.: "Material Balance Calculations with Water Influx in the Presence of Uncertainty in Pressures," SPEJ (June, 1962) 120-128.
3. Tehrani, D.H.: "An Analysis of Volumetric Balance Equation for Calculation of Oil In Place and Water Influx," J. Pet. Tech. (September, 1985) 1664-1670.
4. Wang, B. and Hwan, R.R.: "Influence of Reservoir Drive Mechanism on Uncertainties of Material Balance Calculations," SPE 38918, presented at the 1997 SPE Annual Tech-

nical Conference and Exhibition, San Antonio, Texas, October 5–8, 1997.

5. Walsh, M. P.: "A Generalized Approach to Reservoir Material Balance Calculations," J. Can. Pet. Tech. (Jan., 1995) 55–63.
6. Walsh, M.P.: A Generalized Approach to Petroleum Reservoir Engineering, Petroleum Recovery Research Institute Press, Austin, Tx., 1995.
7. Microsoft Corporation: User's Guide, Excel, Version 5.0, Microsoft Corporation, 1993–94.
8. Petroleum Recovery Research Institute: QUICKSIM: A Modified Black-Oil Model, User's Guide, Version 1.5, Petroleum Recovery Research Institute Press, Austin, Texas, 1999.
9. Galas, C.M.F.: "Confidence Limits of Reservoir Parameters by Material Balance," Paper No. 94-03, presented at the 45th Annual Technical Meeting of the Petroleum Society of CIM, Calgary, Canada, June 12–15, 1994.

## SI Metric Conversion Factors

psi × 6.894 757	E + 00 = kPa
ft <sup>3</sup> × 2.831 685	E-01 = m <sup>3</sup>
bbl × 1.589 873	E-01 = m <sup>3</sup>
ft × 3.048	E-01 = m

## Appendix: Material Balance Equations

**Initially-Saturated Reservoirs.** The material-balance equation, in abbreviated form, for initially-saturated volumetric reservoirs is

$$F = N_{foi}E_o + G_{fgi}E_g \quad (\text{A-1})$$

where  $F$  is the total net fluid withdrawal,  $N_{foi}$  is the original free-oil in-place,  $G_{fgi}$  is the original free-gas in-place,  $E_o$  is the oil phase expansivity, and  $E_g$  is the gas phase expansivity.  $F$  is given by

$$F = N_p \left[ \frac{(B_o - R_s B_g)}{(1 - R_s R_v)} \right] + G_{ps} \left[ \frac{(B_g - R_v B_o)}{(1 - R_s R_v)} \right] + (W_p - W_i)B_w \quad (\text{A-2})$$

Eqns. (A-1) and (A-2) purposely ignore water influx.  $E_o$  and  $E_g$  are defined by

$$E_o = B_{to} - B_{oi} \quad (\text{A-3})$$

$$E_g = B_{tg} - B_{gi} \quad (\text{A-4})$$

$B_{to}$  is the two-phase oil formation volume factor (FVF) and  $B_{tg}$  is the two-phase gas FVF.  $B_{to}$  and  $B_{tg}$  are defined by

$$B_{to} = \frac{B_o(1 - R_{si}R_v) + B_g(R_{si} - R_s)}{(1 - R_s R_v)} \quad (\text{A-5})$$

$$B_{tg} = \frac{B_g(1 - R_{vi}R_s) + B_o(R_{vi} - R_v)}{(1 - R_s R_v)} \quad (\text{A-6})$$

Eqns. (A-5) and (A-6) include  $R_v$ , the volatilized oil-gas ratio.  $R_v$  describes the volatilized-oil content of the reservoir gas phase.  $R_v$  is needed for volatile oils, gas condensates, and wet gases because these fluids naturally contain volatilized oil. The conventional material balance equation ignores  $R_v$ , and as a result, is not applicable to these fluids. The development herein includes this term to purposely broaden the applicability. Eqns. (A-1)-(A-6) follow from the development of Walsh.<sup>5,6</sup>

If we define  $m$  as the ratio of the initial free-gas and free-oil phase volumes, then

$$m = \frac{G_{fgi}B_{gi}}{N_{foi}B_{oi}} \quad (\text{A-7})$$

Solving this equation for  $G_{fgi}$  and substituting the result into (A-1) yields

$$F = N_{foi} \left( E_o + \frac{mB_{oi}E_g}{B_{gi}} \right) \quad (\text{A-8})$$

**Initially-Undersaturated Oil Reservoir.** The material-balance equation for an initially-undersaturated oil reservoir is

$$F = NE_o \quad (\text{A-9})$$

where  $N$  is the total OOIP. For initially-undersaturated oil reservoirs,  $N_{foi} = N$  because there is no initial free gas. While undersaturated,  $F$  and  $E_o$  are given by

$$F = N_p B_o \quad (\text{A-10})$$

$$E_o = B_o - B_{oi} \quad (\text{A-11})$$

While saturated,  $F$  and  $E_o$  are given by (A-2) and (A-3).

**Initially-Undersaturated Gas Reservoir.** The material-balance equation for an initially-undersaturated gas reservoir is

$$F = GE_g \quad (\text{A-12})$$

where  $G$  is the total OGIP. While undersaturated,  $F$  and  $E_g$  are given by

$$F = G_{ps}B_g \quad (\text{A-13})$$

$$E_g = B_g - B_{gi} \quad (\text{A-14})$$

While saturated,  $F$  and  $E_g$  are given by (A-2) and (A-4).

TABLE 1—RESERVOIR PROPERTIES			
<b>General</b>			
Area, acres		3,796	
No. of producing wells		48	
Permeability, md		5	
Oil-leg thickness, ft		20	
Porosity, %		31	
Initial water sat., % PV		20	
<b>Other</b>			
	<b>m = 0</b>	<b>m = 0.25</b>	<b>m = 0.50</b>
Gas-cap thickness, ft	0	5	10
Initial gas-cap gas sat., % PV	80	80	80
OOIP, mmstb	100.0	100.0	100.0
OGIP, Bscf	0	18.98	37.96
OGIP, Bscf	82.0	100.98	119.96

TABLE 2—BLACK-OIL PVT PROPERTIES			
Pressure psia	$B_o$ rb/stb	$B_g$ rb/mscf	$R_s$ scf/stb
1640	1.462	1.926	820.7
1620	1.457	1.951	810.5
1600	1.453	1.977	800.5
1550	1.441	2.047	775.8
1500	1.429	2.126	751.9
1450	1.418	2.211	728.8
1400	1.407	2.305	706.4
1350	1.395	2.406	684.6
1300	1.384	2.514	663.6
1250	1.373	2.630	643.2
1200	1.362	2.753	623.4
1150	1.351	2.884	604.2
1100	1.340	3.023	585.6
1050	1.330	3.169	567.6
1000	1.319	3.323	550.1

TABLE 3—OIL AND GAS PRODUCTION HISTORIES						
Pressure, psia	m=0		m=0.25		m=0.50	
	Prod. Oil mmstb	Prod. Gas Bscf	Prod. Oil mmstb	Prod. Gas Bscf	Prod. Oil mmstb	Prod. Gas Bscf
1640	0.00	0.00	0.00	0.00	0.00	0.00
1620	1.04	0.84	1.36	1.11	1.68	1.37
1600	2.08	1.69	2.74	2.22	3.40	2.76
1550	4.77	3.81	6.30	5.05	7.75	6.28
1500	7.49	5.94	9.67	7.90	11.60	9.84
1450	10.02	8.08	12.47	10.75	14.59	13.38
1400	12.19	10.20	14.68	13.56	16.86	16.89
1350	14.01	12.30	16.44	16.34	18.64	20.36
1300	15.51	14.37	17.88	19.08	20.09	23.77
1250	16.78	16.41	19.08	21.77	21.29	27.12
1200	17.86	18.41	20.10	24.40	22.32	30.39
1150	18.79	20.36	20.98	26.97	23.20	33.58
1100	19.59	22.28	21.75	29.47	23.96	36.68
1050	20.29	24.14	22.42	31.90	24.63	39.68
1000	20.91	25.96	23.01	34.26	25.23	42.58
COIP	100.0 mmstb		100.0 mmstb		100.0 mmstb	
COGIP	0 Bscf		18.98 Bscf		37.96 Bscf	
COGP	82.0 Bscf		100.98 Bscf		119.96 Bscf	

**TABLE 4—TEN RANDOM NORMALIZED PRESSURE ERROR REALIZATIONS**

Normal Distribution Median = 0 Standard Deviation = 1.0 No. of Points per Realization = 15											
	Set 1	Set 2	Set 3	Set 4	Set 5	Set 6	Set 7	Set 8	Set 9	Set 10	Average
1	-0.999	-0.892	0.739	-0.402	0.866	0.344	0.591	0.754	-0.449	0.376	
2	-0.437	-1.156	2.910	0.441	-0.754	-0.601	-0.600	-1.456	0.025	1.053	
3	-1.492	0.451	-0.102	0.866	0.202	0.844	1.091	0.757	-0.512	0.797	
4	0.480	-2.231	0.510	0.596	-0.254	-0.265	-0.887	0.701	1.221	0.633	
5	1.397	-0.518	-1.102	-0.012	-0.603	-0.697	-0.823	2.024	-0.133	-0.752	
6	-1.879	1.879	-1.166	-0.973	1.624	-0.393	0.215	-0.505	-1.265	-0.936	
7	0.696	-0.008	-1.139	-0.815	-0.432	0.599	-1.116	-0.235	-0.293	-0.711	
8	-0.750	-1.002	0.086	0.457	-0.131	0.410	1.248	-0.891	0.791	-0.390	
9	2.178	0.725	0.235	1.008	-0.364	1.192	0.482	0.230	0.401	0.468	
10	0.337	1.679	-2.256	0.207	-0.218	0.170	3.387	-1.407	-0.509	0.199	
11	1.282	-2.321	-0.164	0.437	1.153	0.035	0.635	0.162	0.177	0.218	
12	-1.538	0.543	-0.715	-1.519	0.870	-0.252	0.397	-0.490	0.850	-1.467	
13	1.607	1.206	-2.667	0.408	0.899	-0.650	-1.148	-0.689	0.416	0.774	
14	1.751	-1.606	0.649	-0.100	0.759	-0.063	-0.399	-1.596	-0.104	-1.352	
15	0.956	1.572	-0.980	-1.574	-0.105	-0.152	-0.222	-0.460	-0.043	0.205	
Median	0.239	-0.112	-0.344	-0.065	0.234	0.035	0.190	-0.207	0.038	-0.059	-0.005
Std. Dev.	1.329	1.401	1.351	0.821	0.730	0.559	1.179	0.994	0.634	0.813	0.981
Std. Error	1.284	1.353	1.306	0.793	0.706	0.540	1.139	0.961	0.612	0.786	0.948

**TABLE 5—TEN PRESSURE REALIZATIONS**

Normal Distribution Standard Deviation = 5 psi											
Actual, psia	Set 1	Set 2	Set 3	Set 4	Set 5	Set 6	Set 7	Set 8	Set 9	Set 10	Average
1640	1635	1636	1644	1638	1644	1642	1643	1644	1638	1642	1640.5
1620	1618	1614	1635	1622	1616	1617	1617	1613	1620	1625	1619.7
1600	1593	1602	1599	1604	1601	1604	1605	1604	1597	1604	1601.5
1550	1552	1539	1553	1553	1549	1549	1546	1554	1556	1553	1550.3
1500	1507	1497	1494	1500	1497	1497	1496	1510	1499	1496	1499.4
1450	1441	1459	1444	1445	1458	1448	1451	1447	1444	1445	1448.3
1400	1403	1400	1394	1396	1398	1403	1394	1399	1399	1396	1398.3
1350	1346	1345	1350	1352	1349	1352	1356	1346	1354	1348	1349.9
1300	1311	1304	1301	1305	1298	1306	1302	1301	1302	1302	1303.3
1250	1252	1258	1239	1251	1249	1251	1267	1243	1247	1251	1250.8
1200	1206	1188	1199	1202	1206	1200	1203	1201	1201	1201	1200.8
1150	1142	1153	1146	1142	1154	1149	1152	1148	1154	1143	1148.3
1100	1108	1106	1087	1102	1104	1097	1094	1097	1102	1104	1100.1
1050	1059	1042	1053	1050	1054	1050	1048	1042	1049	1043	1049.0
1000	1005	1008	995	992	999	999	999	998	1000	1001	999.6

TABLE 6—OOIP ERROR: F-vs.-E <sub>o</sub> PLOT		
Pressure Uncertainty, psi	OOIP Estimate, % error	
	y=a+bx	y=bx
0	0	0
5	0.8	1.0
10	1.6	2.0
50	7.4	9.4
100	15.4	16.7
150	26.5	21.4
200	36.6	29.0

TABLE 7—OOIP & OGIP ERROR: F/E <sub>o</sub> -vs-E <sub>g</sub> /E <sub>o</sub> PLOT									
Pressure Uncertainty, psi	m = 0			m = 0.25			m = 0.50		
	% OOIP	% OFGIP	% OGIP	% OOIP	% OFGIP	% OGIP	% OOIP	% OFGIP	% OGIP
0	0	n/a	0	0	0	0	0	0	0
1	21.5	n/a	7.4	28.2	80.5	7.8	34.9	49.8	8.1
2	43.4	n/a	14.8	56.9	162.4	15.7	70.4	100.5	16.4
5	124.0	n/a	42.0	162.6	464.9	44.7	201.2	287.7	46.6

TABLE 8—OOIP & OGIP ERROR: F-vs-(E <sub>o</sub> +mB <sub>oi</sub> E <sub>g</sub> /B <sub>g</sub> ) PLOT									
Pressure Uncertainty, psi	m = 0			m = 0.25			m = 0.50		
	% OOIP	% OFGIP	% OGIP	% OOIP	% OFGIP	% OGIP	% OOIP	% OFGIP	% OGIP
0	0	0	0	0	0	0	0	0	0
1	7.3	n/a	2.6	9.8	27.3	2.8	12.6	17.6	3.0
2	14.7	n/a	5.2	20.4	57.3	5.8	25.6	35.9	6.1
5	37.5	n/a	13.2	49.9	139.9	14.2	56.5	79.2	13.6
10	59.3	n/a	21.0						

TABLE 9—OOIP & OGIP ERROR: PLANAR REGRESSION									
Pressure Uncertainty, psi	m = 0			m = 0.25			m = 0.50		
	% OOIP	% OFGIP	% OGIP	% OOIP	% OFGIP	% OGIP	% OOIP	% OFGIP	% OGIP
0	0	n/a	0	0	0	0	0	0	0
1	7.2	n/a	2.6	9.6	27.0	2.8	12.0	16.8	2.9
2	14.5	n/a	5.2	19.3	54.1	5.6	24.2	33.8	5.8
5	36.4	n/a	12.9	48.4	135.3	13.9	60.4	84.5	14.6
10	71.2	n/a	25.2	94.7	265.1	27.1			

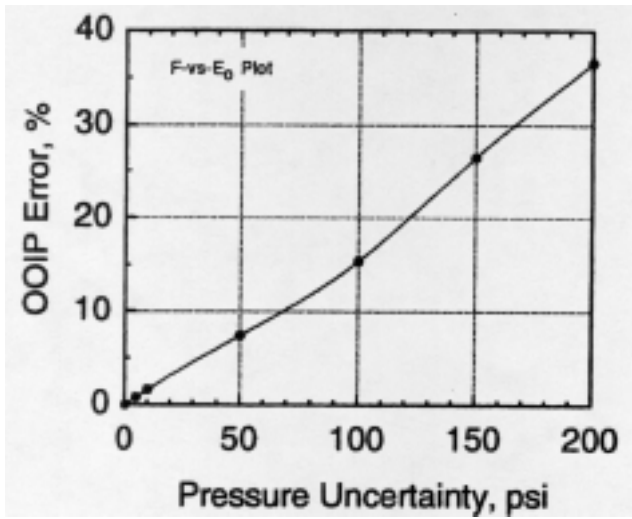


Fig.1 – OOIP percent error as a function of pressure uncertainty for F-vs.-E<sub>0</sub> plot.

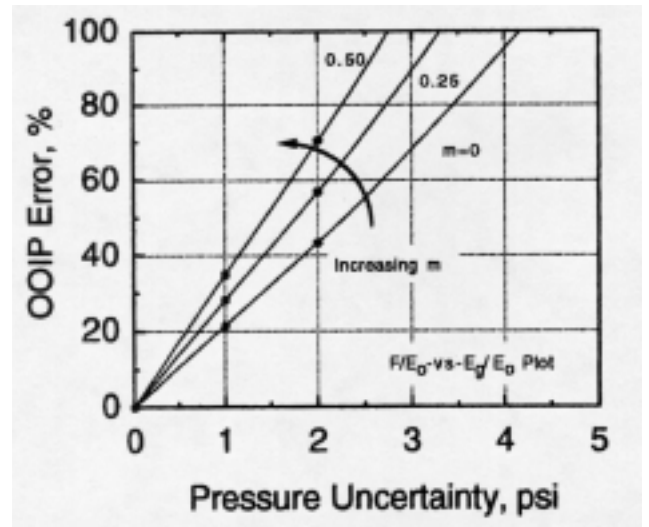


Fig.3- OOIP percent error as a function of pressure uncertainty and gas-cap size for F/E<sub>0</sub> Vs- E<sub>g</sub>/E<sub>0</sub> plot.

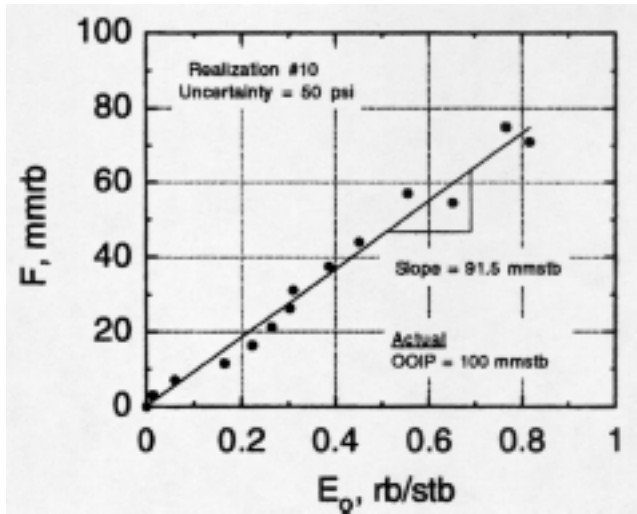


Fig. 2 – Example F-vs. E<sub>0</sub> plot with a 50 psi pressure uncertainty.

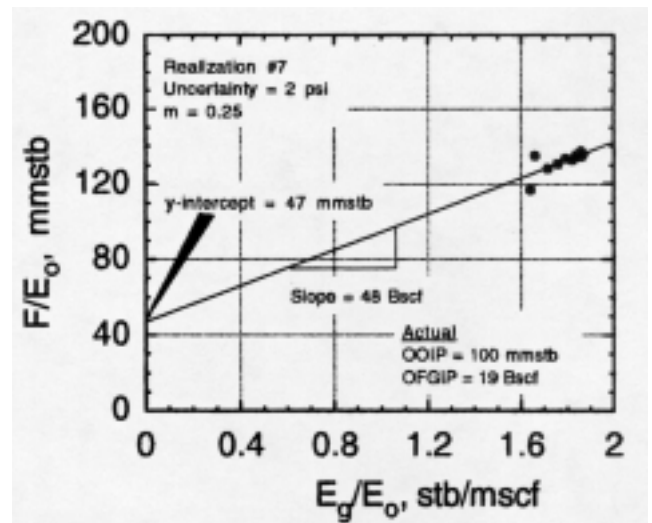


Fig.4-Example F/E<sub>0</sub> vs- E<sub>g</sub>/E<sub>0</sub> plot for a pressure uncertainty of only 2 psi.

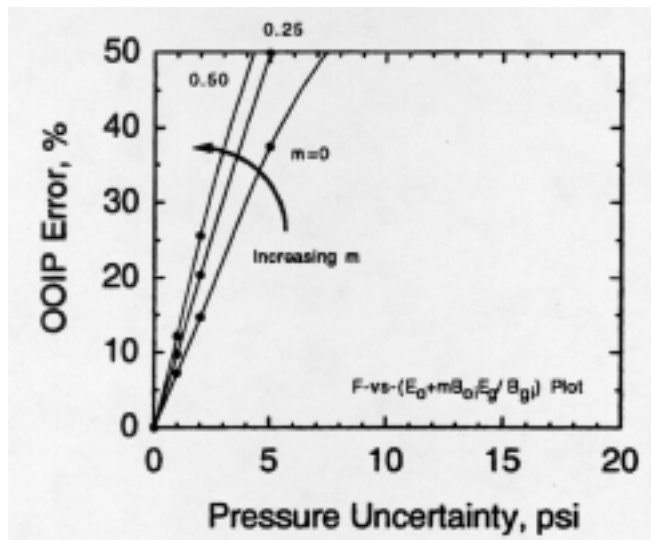


Fig.5- OOIP error as a function of pressure uncertainty and gas-cap size for F-vs.-(E<sub>o</sub> + mB<sub>oi</sub>E<sub>g</sub>/B<sub>gi</sub>)plot.

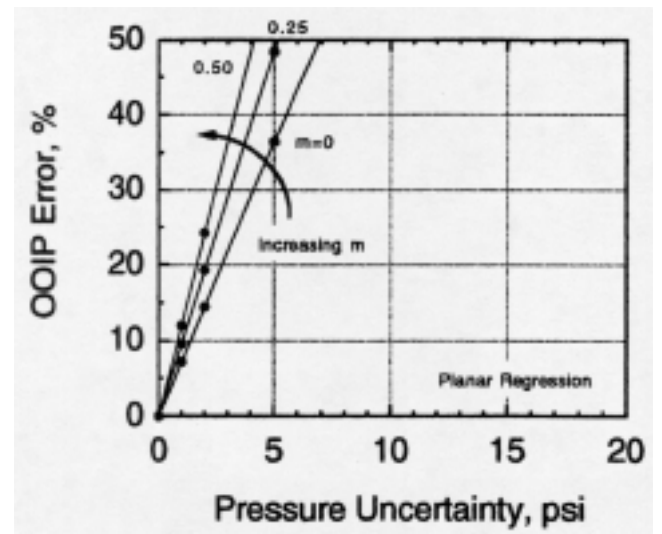


Fig.7- OOIP error as a function of pressure uncertainty and gas-cap size for planar regression.

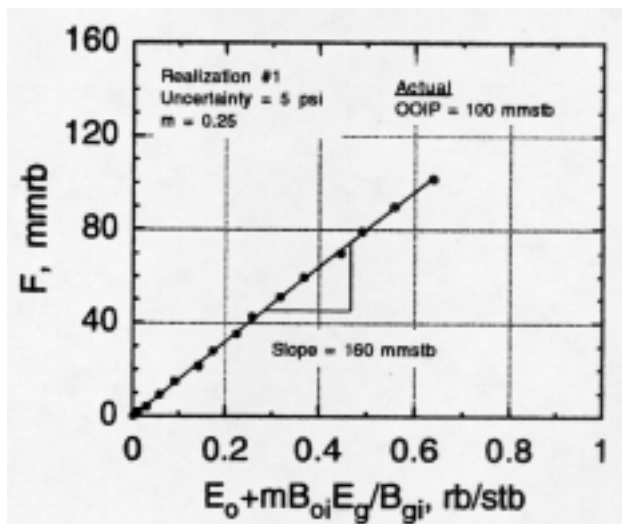


Fig.6- Example F-vs.-(E<sub>o</sub> + mB<sub>oi</sub>E<sub>g</sub>/B<sub>gi</sub>)plot. For a pressure uncertainty of 5 psi.